First-principles study of defect behavior in irradiated uranium monocarbide

R. Ducher,* R. Dubourg, and M. Barrachin
Institut de Radioprotection et de Sûreté Nucléaire, DPAM, SEMIC, LETR, Boîte Postale 3, F-13115 Saint-Paul-Lez-Durance Cedex, France

A. Pasturel
Sciences et Ingénierie des Matériaux et Procédés, INP Grenoble, UJF-CNRS, 1130 rue de la Piscine, Boîte Postale 75, F-38402 Saint-Martin D'Hères Cedex, France and Laboratoire de Physique et Modélisation des Milieux condensés, Maison des Magistères, Boîte Postale 166 CNRS, F-38042 Grenoble Cedex 09, France

(Received 22 October 2010; revised manuscript received 25 January 2011; published 25 March 2011)

Ab initio electron theory based on the projector-augmented-wave method in the generalized gradient approximation of the density functional theory is used for calculating formation and migration energies of point defects in uranium monocarbide (UC). The use of the Hubbard term to describe the 5*f* electrons of uranium is discussed on the basis of the density of states and cohesive energies. A formalism allowing the "raw" calculated energies to be normalized is proposed to take into account the compositional dependence of defective crystals. Such formation energies are then used to determine the population of predominant defects as a function of nonstoichiometry. We identify the most stable defects as uranium antisites and carbon vacancies for UC_{1-x}, and dimers C_2 for UC_{1+x}. The most stable thermal defects are obtained, in turn, by formation of complex defects associating dimer C_2 and carbon vacancies whereas carbon Frenkel pairs and Schottky defects require larger formation energies. The migration energies are also calculated for different mechanisms, using as diffusion vectors both thermal vacancy sources and preexisting constitutional defects in the case of off-stoichiometric alloys. We compare the calculated diffusion paths with available experimental data proposed by Matzke [J. Less-Common Met. **121**, 537 (1986)].

DOI: 10.1103/PhysRevB.83.104107 PACS number(s): 71.15.Mb, 61.72.J−, 66.30.Fq

I. INTRODUCTION

Uranium monocarbide (UC) is considered as one of the promising fuels in the framework of the development of the fourth generation of nuclear reactors, namely, for gas fast reactors but also for sodium fast reactors (whereas UC_2 is often proposed to improve the performance of tristructural-isotropic(fuel)-coated particles for the very-high-temperature reactors). Its many advantages if compared to oxide fuels might explain this interest in uranium carbide. The first one is its very good thermal conductivity corresponding perfectly to one important technological requirement of generation-IV (GENIV) reactors for higher operating temperatures. In addition, also following GENIV reactor requirements, uranium carbide contains a high concentration of metallic elements, allowing high burn-up values (10% or more) to be obtained, and can incorporate significant quantities of plutonium and minor actinides (20%). Finally, UC is stable in its rock-salt structure in a large domain of nonstoichiometry at high temperature, and its fusion temperature is high (2723 K).

As a consequence UC (and mixed carbides) were extensively studied in the past and many experimental investigations were performed. A very exhaustive review of the available experimental data was given by Matzke.[1] From this review, two important problems appear for carbides. They are the significant fuel swelling (mainly by fission gas swelling) and the fission gas release, inducing many serious problems for the thermomechanical behavior of UC fuel.

The in-pile behavior of UC is mainly affected by fission products (including fission gases) and suitable models must be proposed to understand the microstructural behavior. As was demonstrated for UO_2, such models are very dependent on the behavior of the point defects created during in-pile operations.[2–4] Point defects are involved in the formation and behavior of extended defects like dislocations or fission gas bubbles but also in fuel sintering or restructuring, in grain growth, and in the evolution of stoichiometric deviation, and finally they are very important for the incorporation and diffusion of solid fission products. As a first step of understanding the complex behavior of irradiated uranium carbide structure, a very reliable knowledge of the behavior of point defects is thus one key issue.

One important item is the controversial question of diffusion mechanisms of defects in UC. They can be partly explained by spurious effects modifying the kinetics of atomic mobility due to the presence of impurities or of uncontrolled deviations from alloy composition.[5] In polycrystalline structures, the grain boundary diffusion modifies the values of atomic mobility equally. A critical overview of the various sets of values proposed in the literature is presented by Matzke.[1]

From this overview, it is clear that many possible diffusion mechanisms have been suggested for carbon and uranium atoms. For carbon diffusion a vacancy mechanism has often been proposed but tetrahedral interstitial sites and C_2 pairs have been alternatively suggested.[6–11] Important discussions on uranium diffusion mechanisms via either the carbon or the uranium sublattice are also available in many references.[1,8–14]

Regarding these experimental difficulties, one might try to obtain a deeper understanding from first-principles-based calculations. The description of the electronic structure of uranium compounds is known to be a complicated challenge due to the competition between the localization-delocalization and localization-localization effects of the 5*f* electrons of the uranium atoms. Nevertheless, such theoretical approaches were found successful for the study of point defects and

fission products in irradiated UO_2.[15–22] Some studies of bulk properties of UC using similar calculations were recently reported[23,24] but only one[25] was devoted to the point defects and impurities in UC and used density functional theory (DFT) calculations. In that study, the *5f* electrons were assumed to be itinerant and the conventional generalized gradient approximation (GGA) was used for the description of the exchange and correlation potential to calculate the formation energy of defects in the UC structure and the incorporation of He, Xe, and O impurities. As shown by Freyss,[25] the methodological questions are very important and might explain some limitations of such calculations. If some UC properties were well reproduced with the DFT-GGA approach (bulk modulus, lattice parameter, magnetic properties), others are calculated with poor (or at least not satisfying) agreement with available experimental data, like the electron density of states or the formation energy of UC. Freyss suggested that the GGA + U approach with the so-called Hubbard parametric term (U) could be one way to improve the results. Different theoretical studies[23,26] also suggested that the electronic structure of UC could be more properly described by taking into account a partial localization of the *5f* electrons. From the experimental point of view, if the x-ray photoelectron spectroscopy (XPS) and bremsstrahlung isochromat spectroscopy (BIS) measurements[27] on UC seem to show a preponderant itinerant character of the *5f* electrons, they also evidence correlations between these electrons which cannot be completely neglected. The introduction of the Hubbard term was demonstrated to be efficient to treat 5*f* correlation effects in UO_2 for which the GGA approximation did not reproduce its insulating nature.[19] In UO_2, a U value of 4 eV was obtained by fitting the experimental gap occurring in the electron density of states. For UC, a similar approach was also adopted by Shi *et al.*[24] A value of 3 eV for U is chosen to obtain most of the calculated values of elastic constants and phonon dispersion curves in agreement with experimental data, although some discrepancies exist.

In this contribution, particular and important attention will be paid at first to this specific question of the required formalism and the necessity of introducing (or not) the additional Hubbard term. This is done by considering calculations of the formation and cohesive energies of UC as well as a comparison between calculated and available data for the density of states (DOS). Then, in Sec. IV, the results obtained for the formation energies of the different point defects are presented. Some of them are directly comparable to those obtained by Freyss[25] but some additional important point defects are considered. From these results it is possible to propose a list of the most probable defects in the different domains of UC stoichiometry. Defects with low formation energies are of course of prime importance to accommodate the deviation from stoichiometry. Finally, from these most probable defects, the migration energies are calculated for the different domains of stoichiometry and the migration mechanisms obtained are discussed and compared to the experimental data mentioned previously.

These basic investigations are also very useful in the development of the multiscale approaches used to study the solution of fission products (FPS) and the microstructural behavior in carbides as was done previously for oxide fuels in collaboration between IBRAE (Russian Academy of Science, Moscow) and IRSN (French Institute of Radioprotection and Nuclear Safety, Cadarache).[28]

II. METHODOLOGY

In the present paper, density functional theory calculations of total energies were performed with spin polarization using the projector-augmented-wave[29] method as implemented in the Vienna *ab initio* simulation package (VASP).[30]

Most of the calculations, namely, the ones related to the determination of the defect energies and the migration energies of defects, were done with the generalized gradient approximation for the exchange-correlation potential as parametrized by Perdew and Wang (PW91).[31] Calculations are performed using the $6s^2$,$6p^6$,$5f^3$,$6d^1$,$7s^2$ uranium electrons and $2s^2$,$2p^2$ carbon electrons as valence electrons. One-half of the atomic distance between nearest neighbors was systematically controlled to be greater than the cutoff radii of the augmentation spheres (1.208 and 0.699 Å for uranium and carbon, respectively) in order to avoid spheres overlapping, especially in the case of antisite and interstitial defects where interatomic distances are relatively reduced. The GGA + U approximation was also used in order to investigate the influence of the localization of the *5f* electrons of uranium atoms [already identified as crucial in the studies of the electronic structures of some uranium compounds such as UO_2 (Ref. 19)] on the density of states of UC and on its cohesive energy. Within this framework, the localized electrons (5*f*) experience a spin- and orbital-dependent potential, while the other orbitals are delocalized and considered to be correctly described by the GGA approximation. The rotationally invariant form of the GGA + U approximation was used with a spherically averaged double counting term. Within this approach, there is one single parameter, which will be called U_{eff}. In all the calculations, the cutoff energy for the plane wave basis was set to 400 eV for both uranium and carbon.

For the calculation of formation energies of point defects in UC, a 64-atom supercell ($U_{32}C_{32}$) was used. Numerical integrations were performed by sampling the Brillouin zone with a $4 \times 4 \times 4$ Monkhorst-Pack k-point mesh in order to minimize the differences of total energies. Convergence was assumed to be reached when residual forces acting on atoms were less than 10^{-3} eV/Å. The atomic positions and the cell parameter were first optimized from the relaxation cycle for the perfect crystal in the supercell configuration. For supercells that contained point defects, only the atomic positions were relaxed while the cell parameter was kept equal to the equilibrium value for the perfect supercell. Calculations of the energies of pure uranium and carbon solids in their reference states at 0 K (α-U and carbon graphite, respectively), required to determine the point defect energies, were obtained with the spin-polarization GGA approximation, on four-atom simple cells and an $11 \times 11 \times 11$ k-mesh sampling of the Brillouin zone. The structural optimization were carried out in a relaxation cycle involving both atomic position and cell parameter optimization. The calculated energies estimated by subtracting the spin-polarized atomic energy of U and C, respectively, are 6.85 eV/atom for α-U and 7.97 eV/atom for carbon graphite [to be compared to the experimental values, 5.55 eV/atom and 7.37 eV/atom (Ref. 32)].

Finally, migration energies of defects were estimated from the nudge **e**lastic **b**and (NEB) method[33] as implemented in VASP.

III. ELECTRONIC DENSITY OF STATES AND COHESIVE ENERGY

A. DFT-GGA calculations

As mentioned in the Introduction, the previous DFT studies[24,25] evidenced that some controversy still exists about the choice of the more adequate approximation for the exchange-correlation potential (GGA or GGA + U) in the calculations for the description of the electronic structure of UC. In a first step, we have chosen to use the GGA approximation. Within this approach, we calculated the total energy of UC (NaCl structure) by varying the lattice constant in order to determine the equilibrium value. The calculated value was 4.93 Å to be compared to the experimental value[34] (4.96 Å), i.e., an underestimation of 0.6% by the calculation. The calculated cohesive energy obtained by subtracting the spin-polarized atomic energies of U and C from the total energy of UC is equal to 15.12 eV/UC molecule, i.e., a relative error of 8.4% in comparison with the experimental value[35] (13.95 eV). This difference may appear to be relatively small. Nevertheless, the experimental cohesive energy of UO_2 is reproduced by the DFT-GGA calculations with a smaller relative error of 3%.[19] Another way to evaluate the magnitude of the error of the calculation on UC is to calculate the formation enthalpy of the compound. The formation enthalpy is straightforwardly estimated from the calculated cohesive energy of UC (15.12 eV) and the experimental cohesive energy values for α-U (5.55 eV) and for carbon graphite (7.37 eV). A value of 2.2 eV is finally obtained, i.e., more than twice the assessed experimental value[35] (1 eV/UC). (In this estimation, the experimental values for pure solids are preferred to the calculated ones because the errors on the DFT-calculated cohesive energies of this compound are of the same order of magnitude as that on the UC cohesive energy; if the calculated values are used, an enthalpy of formation of 0.3 eV is obtained but leads to a fictitious reduction of the absolute error.) This disagreement in the cohesive energy may be attributed to the possible inability of the conventional GGA to treat the electronic structure of the compound, in particular the f electrons of uranium atoms (see the next section) but also to some errors introduced by the calculations of the energies of the isolated atoms. In particular, it can be shown that the ground state of the uranium atom calculated in the GGA differs from the configuration for which the pseudopotential was generated. In the GGA, the calculated shell occupancy was $5f^4 6d^{3.2} 7s^{0.8}$ whereas the PW91 pseudopotential for the uranium atom is derived from the experimental ground state $5f^3 6d^1 7s^2$. It leads to a difference which can be evaluated as 2.8 eV/atom.

On Fig. 1, the calculated curve of the density of states is shown (full line, with $U = 0$) and compared to the experimental one (dashed line) determined by XPS and BIS techniques.[27] The most remarkable features are the presence of an intense peak below the Fermi level at a binding energy of 0.6 eV and a reduced density of states near the Fermi level (which is a possible indication of the usually assumed semimetallic character of UC). Above the Fermi level, in the excited-state region, the experimental DOS is mainly characterized by one peak at 1.5 eV. The calculated DOS is very similar to the one obtained by Shi *et al.*[24] but neither the peak below the Fermi level at 0.6 eV nor the reduction of the density of states near the Fermi level observed on the experimental curve are reproduced in DFT-GGA calculations. The theoretical DOS above the Fermi level is no longer consistent with the experimental data even; one must consider that the unoccupied states are usually poorly described by the DFT approach. The projected DOSs for the different orbitals (not reproduced in this paper; see Ref. 24) show that the U $5f$ electron states lie in a relatively broad band crossing through the Fermi level (from -5 to $+5$ eV), implying a dominant effect of these electrons on the cohesive properties of the UC compound. The U $5f$ states mainly hybridize with the C 2p states (in agreement with the results of Trygg *et al.*[26] obtained from the full-potential linear muffin-tin orbital method).

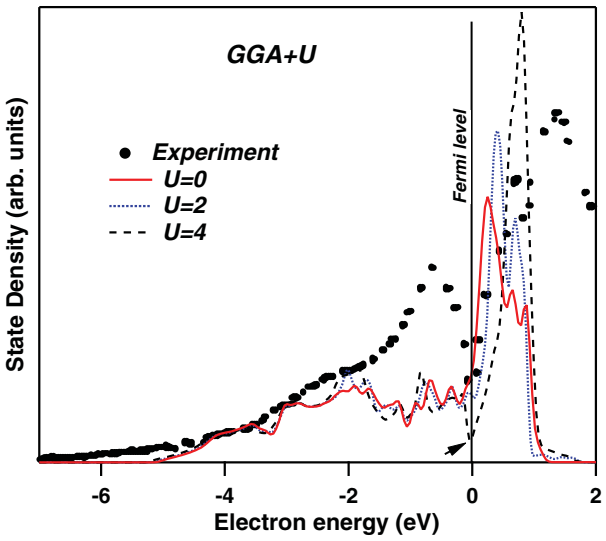

FIG. 1. (Color online) Density of states of UC calculated by GGA + U method for different values of the U term. Dotted line corresponds to the experimental points extracted from the work of Ejima *et al.* (Ref. 27).

B. DFT-GGA + U calculations

Considering the disagreements evidenced in the previous section between the calculated values in the GGA approximation and the experimental data on the cohesive energy and the DOS, we chose to use the spin-polarized GGA with the Hubbard correction term (GGA + U); this is known to possibly improve the description of the localization of the $5f$ electrons of the uranium atoms, which is generally suspected in uranium compounds.[36]

As was previously done by Shi *et al.*,[24] the value of U_{eff}, the single parameter of the approximation, was tuned in order to try to obtain a better description of the different UC bulk properties experimentally investigated. For different values of U_{eff}, the calculated values of the lattice parameter and cohesive energy are reported in Table I. As expected within the GGA + U approximation, an increase of U_{eff} leads to an increase of the lattice parameter, and is then in better agreement with the

TABLE I. Calculated and experimental lattice parameters and cohesive energies for different values of the Hubbard potential.

GGA	Lattice parameter (Å)	Corrected cohesive energies (eV)
$U = 0$	4.93	15.12
$U = 1.05$	4.95	14.28
$U = 2.05$	4.96	13.02
$U = 3.05$	4.98	12.85
$U = 3.55$	5.00	12.46
$U = 4.00$	4.98	12.11
Experiment	4.96	13.95

experimental value for U_{eff} between 1 and 2 eV. Regarding the cohesive energy, the different GGA + U calculations seem to converge toward the experimental value (13.95 eV) for U_{eff} between 1 and 2 eV. In their study, Shi *et al*. considered a different value of 3 eV for U_{eff}, which was chosen as a compromise in order to correctly reproduce the experimental data related to the elastic constants, the lattice parameter, and the bulk modulus. However, Shi *et al*. did not manage to reproduce the C_{12} elastic constant for any value of the Hubbard potential.

In this study, the density of states was calculated for different values of U_{eff} (Fig. 1). In the region beyond the Fermi level, in unoccupied states, we observe large discrepancies between experimental and theoretical curves whatever the value of the Hubbard potential used. By contrast, in the region of occupied states, the introduction of a U_{eff} potential (with a value at least equal to $U_{\text{eff}} = 4$ eV) results in a significant reduction of the density of states at the Fermi level (at the location indicated by the arrow in Fig. 1), i.e., in qualitative agreement with the experimental curve. Nevertheless, the experimental intense peak below the Fermi level is not reproduced in the calculation.

At this stage, on the basis of the lattice parameter and the cohesive energy calculations, the comparison between the results obtained in both GGA and GGA + U schemes seem to be in favor of a (partial) localization of the f electrons of uranium atoms in the UC compound but the use of the Hubbard potential is not sufficient to have a correct description of the main features of the DOS of UC. For that reason, the calculations of the point defect characteristics presented hereafter will be performed in the GGA approximation.

IV. DEFECT FORMATION ENERGY

A. Single point defects

In his work Freyss[25] considered only the formation of vacancies and interstitials as single point defects despite the key role which might be played by antisite defects in diffusion processes, as will be shown later.

The usual expression for the calculation of the formation energies of one vacancy (Vx) or one interstitial defect (Ix) (where x labels uranium or carbon defect), $E^F_{Vx,Ix}$, is

$$E^F_{Vx,Ix} = E^{N\pm1}_{Vx,Ix} - E^N \pm E_x, \tag{1}$$

where E^{N-1}_{Vx} and E^{N+1}_{Ix} are the energies of a supercell containing one vacancy Vx and one interstitial Ix, respectively, E^N the energy of a perfect crystal (with N atoms), and E_x the energy of a uranium or carbon atom in its respective reference state (the reference states of the elements are their solid pure states at ambient temperature, i.e., graphite carbon and α-uranium).

For the antisite, the formation energy must be expressed differently. If we consider a crystal constituted of two sublattices (the first one occupied by the A-type atoms and the second one by the B-type atoms) the antisite formation which consists in removing a B atom from its current position and replacing it by an A atom leads to the following expression for the antisite defect formation energy $E^F_{A_B}$:

$$E^F_{A_B} = E^N_{A_B} - E^N - E_A + E_B, \tag{2}$$

where $E^N_{A_B}$ corresponds to the energy of the supercell containing atom A in the antisite position on the B sublattice, E_A and E_B being the energies of the reference states of the A and B atoms, respectively.

The energies of formation of all single point defects considered here are displayed in Table II as well as values obtained by Freyss. The two sets of values are in agreement. We find that the energy for a dimer defect oriented along the direction ⟨001⟩ is +0.7 eV lower than for the two ⟨111⟩ and ⟨110⟩ orientations studied by Freyss. The ⟨001⟩ orientation considered in our calculation for C-C binding has not been mentioned previously to our knowledge. Bonding effects between uranium and carbon atoms seem to contribute to the stabilization of the C_2 dimer along the ⟨001⟩ direction. Nevertheless, the stabilization of the ⟨001⟩ orientation for C-C could be destabilized by thermal effects since orientations leaving more space for the dimer to vibrate could be preferred. Our findings establishing a relatively low energy cost of inserting the dimer C-C inside the carbon octahedral sites agree very well with the structural study[37] which effectively demonstrated that overstoichiometry can be related to the occurrence of C_2 dimers. A second important result of this study is the amount of energy required to place a uranium atom on the antisite position. The comparison of this value

TABLE II. Calculated formation energies of defects (eV/atom) and comparison with Freyss's calculations (Ref. 25).

	Energy of defect formation (this study)	Freyss
Carbon interstitial	2.62	2.56
Dimer C_2 ⟨001⟩	1.34	–
Dimer C_2 ⟨110⟩	2.23	2.16
Dimer C_2 ⟨111⟩	2.28	2.18
Uranium vacancy	4.62	4.55
Carbon in antisite	9.33	
Carbon vacancy	0.81	0.83
Uranium in antisite	0.88	
Uranium in antisite + carbon vacancy	1.62	
Uranium interstitial	3.01	3.03
Dimer U_2 ⟨111⟩		2.18

with the formation energy of a carbon vacancy shows that the antisite defect can play an important role as a constitutional defect in understoichiometric alloys. No experimental feature in UC, however, proves the existence of antisite atoms in the understoichiometric regime. Competing with this defect, Freyss[25] suggests the possibility that stable uranium dimers are formed with ⟨111⟩ orientation. From Table II, this defect is, however, less stable than uranium located in the antisite.

B. Relative stability order of single point defects

If we consider the off-stoichiometric domains and more particularly the overstoichiometric region which is of interest in the irradiation regime, it appears that the expressions (1) and (2) are not completely suitable to determine the defect population stability insofar as they do not take into account the composition deviations generated by the introduction of defects within the supercell considered in the calculation. In other words, it is hazardous to compare formation energies of defects if the defects lead to very different concentration deviations from the equimolar composition (UC).

To define the stability order of the defects in the different composition domains, we have followed another approach. The basic idea of this approach, already used in previous studies,[38,39] is to consider the formation energies of structures rather than the formation energies of defects.

The formation energy of a supercell with one defect (*def*) (of any type), ΔE^F_{def}, is calculated using the following classical equation:

$$\Delta E^F_{\text{def}} = \frac{N}{n+m} E^{n+m}_{\text{def}} - \left(\frac{n \times N}{n+m}\right) E_{C\,gr.} - \left(\frac{m \times N}{n+m}\right) E_{U\,\alpha} \tag{3}$$

where E^{n+m}_{def} corresponds to the energy of a supercell with one defect. The reference energies are weighted by the atomic fractions $[n/(n+m)]$ and $[m/(n+m)]$ of carbon and uranium, respectively, and N is the number of atoms in the nondefective supercell. The parameters n and m vary according to the nature of the defect. For example, starting from an initial nondefective supercell of $N = 64$ atoms, n and m will be equal to 31 and 32, respectively, for one carbon vacancy, 32 and 33 for one uranium in the interstitial position, and 31 and 33 for one defect antisite of U type. Two remarks can be made about Eq. (3): As this expression is normalized by $(n+m)$, it gives energies ΔE^F_{def} of different defects referred to the same total atom number N. This allows us to make comparisons on the same basis with the nondefective supercell. Excepted for the supercell containing one atom in the antisite position, we remark that the number of defects considered in the expression (3) is not strictly equal to 1 but to the incomplete fraction of defects whose value imposed by the renormalization is equal to $64(n+m)$.

In Fig. 2, ΔE^F_{def} values of the different defective supercells are reported versus the carbon composition. As previously mentioned, it can be immediately seen that the introduction of one defect of one type in the initial nondefective supercell ($N = 64$) creates a deviation from the equimolar composition depending on the nature of this defect. For example, for the supercell containing one antisite defect (circles), the composition deviation is twice higher than those produced

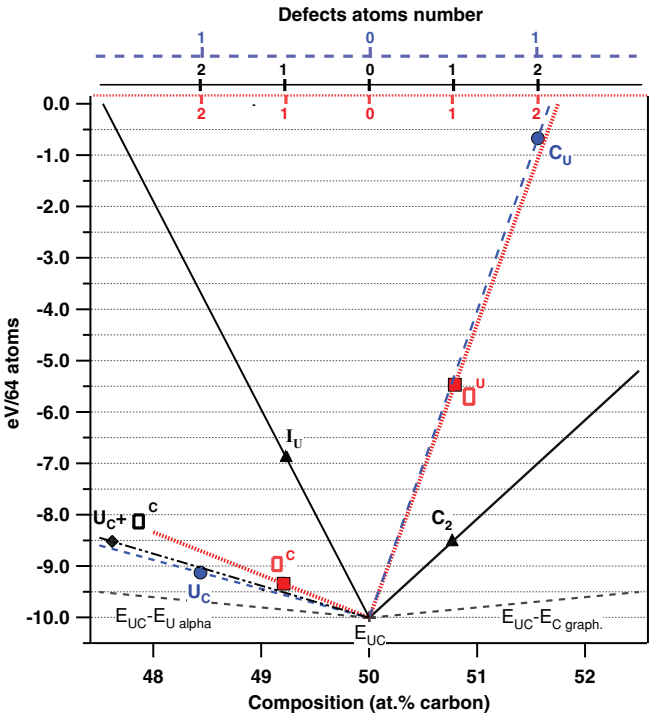

FIG. 2. (Color online) Formation energies of UC alloys as a function of supercell composition (bottom scale) and number of defects (top scale). At the top, dotted, solid, and dashed axes correspond respectively to vacancy, interstitial, and antisite defects. In the notation □ is for vacancy, C_2 for dimer, and A_B for antisite defect with the letter in the subscript corresponding to the nature of the sublattice where the element is in the antisite.

by the creation of a vacancy (squares) or by the introduction of an interstitial (triangles), these latter two being roughly equivalent.

To compare the relative stabilities of the supercells containing different types of defects, we assume that the formation energy of the defective supercell is a linear function of the defect concentration (or of the carbon composition). The linear dependence can be considered as a reasonable assumption if the different defects do not interact (Freyss[25] showed that the minimal size of supercell required to have noninteracting point defects must be at least 64 atoms). Within this assumption, we can directly deduce for one given carbon composition the relative stability of the different defective structures from the slopes of the branches that connect the *formation* energy corresponding to the defective structures ΔE^F_{def} to the *formation* energy corresponding to the UC nondefective structure ΔE^F_0 defined by an equation analogous to (3):

$$\Delta E^F_0 = \frac{N}{n+m} E^{n+m}_0 - \left(\frac{n \times N}{n+m}\right) E_{C\,gr.} - \left(\frac{m \times N}{n+m}\right) E_{U\,\alpha}, \tag{4}$$

where n and m are both equal to $N/2$ and E^{n+m}_0 is the energy of the UC perfect crystal.

In the overstoichiometry region, we can see from Fig. 2 that the energy associated with the formation of alloys containing defects of C_2 dimer type is the lowest one. This result does not change the concluding remarks deduced from Table II. From

this result, it is shown that the overstoichiometry can be related to the occurrence of C_2 dimers as observed in experimental crystallographic studies.[37] The possibility that a second carbon atom can be inserted into octahedral sites can be explained by the small size of these atoms and the low compactness of the UC crystal.

In the understoichiometric region, calculations have been performed for single point defects and for clustering defects associating a uranium antisite and a carbon vacancy in first-neighbor positions. Concerning the single defect, the two lowest branches correspond to the uranium antisite and the carbon vacancy. These two branches being relatively close, it is interesting to check whether the interaction between vacancy and antisite in first-neighbor positions is attractive or not. Calculations show that the energy of this cluster (uranium antisite + carbon vacancy) is lower than the energies of the two single defects considered separately. We can conclude that uranium in the antisite position, combined or not with a carbon vacancy, appears as the dominant defect in the understoichiometric region. The presence of antisite atoms in the UC structure is comparable with what occurs for the nickel-rich part in the NiAl structure.[38,39] To our best knowledge, the uranium antisite is not mentioned in the literature on UC as a constitutional defect; only the carbon vacancy is considered in the understoichiometric region. However, the interpretation of the present calculations has to be taken cautiously because the conclusions could be modified by the introduction of entropic effects. Indeed, Fig. 2 shows that none of the defective alloys is stable at 0 K since all associated branches are situated above the stable branches connecting lateral pure solid states with the perfect crystal UC (shown in dotted lines on Fig. 2). It agrees very well with the U-C phase diagram at low temperature. As discussed previously, the relative stabilities of alloys can be extrapolated at finite temperature only if the evolution of the free enthalpy with temperature of the defective structures does not change the stability order deduced from the formation enthalpies calculated at 0 K. We suspect that the configurational entropy evolves differently, depending on the nature of the defect. For instance, considering that the vacancy concentration has to be twice higher than the antisite concentration to accommodate the same carbon concentration, the configurational entropy term of structures with vacancy-type defects should be higher than that of structures with antisite defects. Thus, in the understoichiometric region we cannot exclude the idea that the carbon vacancy could be favored as the temperature increases. For the overstoichiometric region, the entropic terms are less important since the C_2 dimer curve is much lower than other curves.

From our formalism, it is also possible to define the formation energies of defects. The formation energy of a defect, E_d, is simply deduced from the linear expression relating the formation energy of the defective alloy, ΔE^F_{def}, and the defect concentration x_d:

$$\Delta E^F_{\text{def}} = \Delta E^F_0 + E_d x_d. \tag{5}$$

E_d represents the slopes of the segments reported in Fig. 2 but by considering the x axis reported on the top of the figure. Because of normalization effects introduced by Eq. (5), the E_d values reported for the different defects in Table III are slightly different from the values of Table II.

TABLE III. Formation energies of defects (eV/atom) calculated from the expression (5).

	Energy of defect formation (this study)
Dimer C-C	1.50
Uranium vacancy	4.46
Carbon in antisite	9.33
Carbon vacancy	0.65
Uranium in antisite	0.88
Uranium in antisite + carbon vacancy	1.46
Uranium interstitial	3.17

C. Composition-conserving defects

In off-stoichiometric regions, as for stoichiometric composition, the formation of thermal defects is governed by the composition-conserving rule which states that the introduction of thermal defects must not modify the alloy composition. To respect this condition, the composition-conserving defects must be generated at least by pairs of single point defects and can take in some case complex forms when several single defects are implied. For example, we can consider the creation of a defect cluster formed by one atom A in an antisite on the B sublattice and, to compensate the deficit in B atoms, by a bivacancy on the A sublattice. This type of defect, called a triple defect, is often selected in the list of potential defects, as what done by Korzhavyi *et al.*[38] for NiAl. For UC, we can estimate in first approximation from the energies of single defects expressed in Table III that even if the formation energy of the uranium antisite defect is low, the cost for forming two uranium vacancies is too prohibitive for this to be considered as a possible defect. Similarly, the carbon antisite requires a too large energy to be considered as a serious alternative in a complex defect with a carbon bivacancy even if the energy to form the carbon vacancy is in comparison very low. Other complex associations including dimers will be investigated in the following because of their low formation energy.

Concerning the pair clustering defects, there are two common types: Frenkel pairs corresponding to A or B interstitial-vacancy couples and Schottky defects resulting from the association of A and B vacancies. A less conventional defect based on the capacity of octahedral sites to incorporate the dimer C_2 is suggested for UC. The creation of this dimer must be coupled to the formation of a carbon vacancy to preserve composition.

In addition to the usual defects of Schottky and Frenkel type as investigated by Freyss,[25] we will also consider thermal defects involving the dimer C_2 as well as those included in pair defects and those in triple defects.

1. Frenkel defects

Frenkel defects are of two types: carbon and uranium Frenkel pairs. In both cases, their energies result (Table IV) from the sum of the formation energies calculated for isolated

TABLE IV. Thermal defect formation energies (eV) (in the GGA approximation).

Defect type	Frenkel C	Frenkel U	Schottky	$C_2^{[100]} + \square^C$	$U_C + 2C_2$
Formation energy	+3.4	+7.6	+4.3	+0.9	+3.9

vacancy and interstitial point defects. Indeed, direct calculations with interstitial and vacancy defects in first-neighbor positions show that the interstitial atom returns to its original position irreversibly with atomic relaxation on the uranium sublattice in the absence of an energy barrier between the interstitial and octahedral positions. The formation energies for Frenkel pairs defined from isolated point defects are reported in Table IV. Freyss's values for Frenkel pairs with unbounded point defects are strictly identical to our own values. Freyss also calculated the energy of Frenkel pairs with uranium forming a dumbbell rather than placed in tetrahedral sites. His results show that this configuration stabilizes the Frenkel defect somewhat more (around 0.7 eV) than if it was in the tetrahedral position. However, this defect remains very costly to form, which disqualifies it as one of the possible vectors for the diffusion of uranium atoms in the cell. Schottky defects are more promising because of their relatively low energy.

2. *Schottky defect*

For Schottky defects, the energy value of +4.3 eV proposed in Table IV is calculated from the real configuration, i.e., with uranium and carbon vacancy defects positioned in the nearest-neighbor position along the ⟨100⟩ direction, and not from the isolated defect as was done for the Frenkel defect. This value is lower by about 0.8 eV than the sum of the energies of the corresponding isolated defects and suggests a stabilization effect of uranium and carbon vacancies when placed as first neighbors. This point agrees very well with calculations performed by Freyss.[25] All calculations tend to demonstrate that the Schottky defect is the thermally activated defect by which uranium atoms can move in the stoichiometric compound.

3. *Dimer C_2 plus carbon vacancy*

A view of this complex defect is proposed in Fig. 3 where an image of the (001) plane is traced showing the dimer C_2 along the ⟨001⟩ direction and a carbon vacancy separated from it by a uranium atom. The results presented in Table IV underline the relatively low energy required to create dimer plus carbon vacancy defects (+0.9 eV) compared to the energies required for the formation of Schottky (+4.3 eV), carbon Frenkel pair (+3.4 eV), or uranium Frenkel pair (+7.6 eV) defects. This defect might be considered as the most stable, in good agreement with the thermodynamic calculations performed by Jeanne[40] leading to the same conclusion. Association between one carbon vacancy and the ⟨001⟩ C_2 dimer is more favorable than if a carbon interstitial occupied the tetrahedral site as happens in classical Frenkel defects. In addition, we note that the energy of this bidefect is lower when the vacancy and dimer are bound and aligned along a common ⟨100⟩ direction. The stable ⟨100⟩ orientation agrees with that calculated previously for a dimer single defect without vacancy.

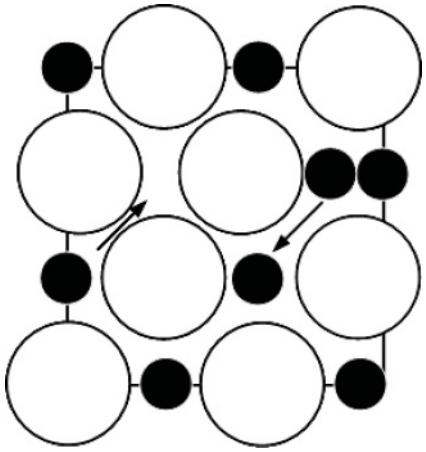

FIG. 3. Double diffusion paths in stoichiometric UC alloy [view of UC (001) plan: in white, U atoms, and in black, C atoms].

4. *Triple defect*

The low formation energy of C_2 dimers may induce the creation of more composition-conserving defects. One possible association to consider is that of uranium in an antisite with two dimers C_2. The total energy for this clustering defect is about +3.9 eV (this energy does not take into account the possible interactions between defects). Note that this energy is about 0.4 eV less than the energy needed to create a Schottky defect, which makes this defect a likely mechanism for the diffusion of uranium in the UC crystal in the expectation of low migration energy of uranium atoms. This is the subject of the next section.

V. CARBON AND URANIUM MIGRATION ENERGIES

From the previous calculations, it is possible to propose a set of defects (single or complex) able to accommodate off-stoichiometric compositions. The diffusion mechanisms will be investigated on this basis, considering both the formation energy of defects and the migration energy of species using these defects as vectors for diffusion in the lattice.

A. Carbon migration

The likely mechanisms for carbon atom diffusion have been investigated and the results are reported in Table V. The results given here are based on calculations performed on single point defects, using the nudge elastic band method. For a diffusion path implying complex defects, the migration energy is calculated from isolated single defects without taking into account the influence of other cluster defects in the migration mechanism.

TABLE V. Defect migration energy (eV) calculated for carbon for the most likely single point defects.

Defect	Vacancy	Interstitial	C_2 (oct.) → C (oct.)
Migration energy	+2.0	+1.6	+1.6

1. Stoichiometric composition

In stoichiometric UC, as shown previously, the C_2 dimer associated with a carbon vacancy is the most stable defect. Its formation energy was calculated to be 0.9 eV. It is the defect from which C migration might be investigated according to two possible pathways as shown in Fig. 3.

The first one considers carbon atom diffusion through a carbon vacancy. The second one can occur by an interstitial mechanism consisting in moving the carbon atom from an octahedral site with double occupation toward an adjacent site with single occupation. For the former, the migration energy needed for carbon to jump to a neighboring carbon vacancy position is equal to +2.0 eV (see Table V). For the latter, the calculated energy is +1.6 eV. The migration energies for the two mechanisms are not too different. Moreover, these two mechanisms appear in some ways to be combined mechanisms. Indeed, because of the stabilizing effect between the dimer and adjacent carbon vacancy, we can imagine that both processes are involved simultaneously to keep vacancies and dimers in adjacent positions. The mechanism with highest energy constitutes thus the limiting process to carbon diffusion. Thus, for stoichiometric composition, the activation energy for carbon diffusion is given as the sum of the energy required to create the dimer plus carbon vacancy (+0.9 eV) and the energy calculated for the migration of the carbon atom via carbon vacancies (+2 eV). This energy is 2.9 eV, in good agreement with experimental values given by Wallace *et al.*,[41] (+2.8 eV) Krakowski,[42] (+2.8 eV) and Bertaud[43] (+2.9 eV).

2. Understoichiometric composition

Understoichiometry in UC is mainly related to the association of a uranium antisite with a carbon vacancy as first neighbors as obtained in the previous section. We can estimate that the diffusion of carbon occurs through carbon vacancies of the bidefect as illustrated by the arrow in Fig. 4.

In this case, the activation energy corresponds to the carbon diffusion from an occupied site toward the adjacent vacant octahedral site only. As mentioned previously, the influence of uranium in the antisite during the migration of the carbon atom is not considered here. This energy is then estimated from Table V to be +2.0 eV.

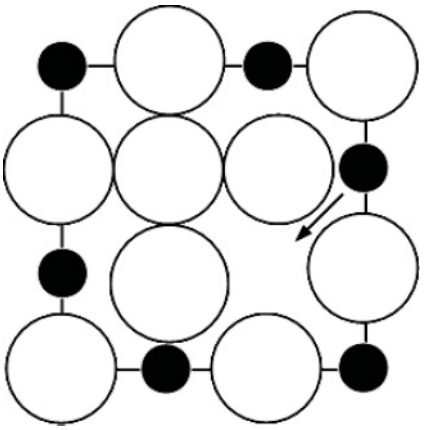

FIG. 4. Diffusion path for carbon atom in understoichiometric alloy with uranium in carbon sublattice.

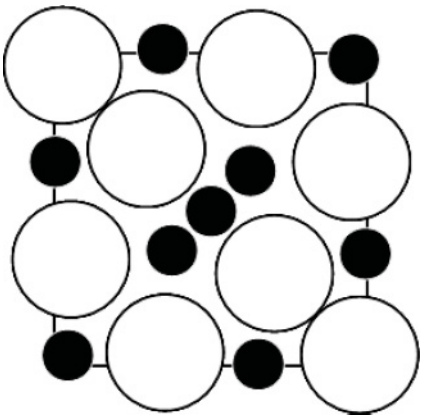

FIG. 5. Position of carbon atom in middle of diffusion path (saddle point).

In addition, as temperature increases, additional defects are thermally created and might participate in the diffusion of carbon atoms through a mechanism similar to those proposed for the stoichiometric composition. This could explain why two sets of values are found in the literature: The first set with energy around 2.1 and 2.4 eV (Refs. 7, 44, and 45) will correspond to the vacancy-based mechanism obtained at low temperature. For the second set, the energy is estimated according to the authors as between 3.3 and 3.7 eV, which is slightly higher than our values obtained using thermal defects (see Sec. V A 1).

3. Overstoichiometric composition

For the overstoichiometric regime, defects formed by dimers in octahedral sites are dominant in the crystal according to the calculation presented in Table III. These defects being pre-existing, the activation energy of carbon is simply equal to the migration energy necessary to move an atom from an octahedral site with double occupation to an adjacent site. The energy barrier was estimated previously to be about +1.6 eV. This mechanism is illustrated on Fig. 5 by a scheme representing the moving atom in the saddle-point position. This value is slightly lower than the experimental value obtained by Makino *et al.*[7] in measurements carried out in the range of C:U ratio between 1.02 and 1.52, namely, 2.3 eV.

All the results obtained for carbon diffusion are in very good agreement with the conclusions from the works of Sarian[6] and Jeanne,[40] who investigated the carbon migration mechanism in uranium monocarbide for the different ranges of composition in the UC phase domain.

B. Uranium migration

Various mechanisms are proposed in the literature for uranium diffusion in UC, based on diffusion via either the carbon or the uranium sublattice. In this section the results of our calculations investigating the different diffusion paths mentioned in the literature for the different regimes of composition are presented.

TABLE VI. Defect migration energy (eV) calculated by NEB method for uranium for the most likely single defects of UC.

Defect	Vacancy	Interstitial	$U_C \rightarrow \square_C$
Migration energy	+1.8	+3.0	+2.7

1. Stoichiometric composition

For stoichiometric composition, the migration energies calculated for the different mechanisms proposed in the literature are gathered in Table VI:

(a) First the migration path commonly proposed in previous experimental work[11] assumes that uranium diffusion occurs through vacancies of the uranium sublattice. To preserve composition, uranium vacancies are treated in the framework of Schottky defects. The migration energy calculated by the NEB method for uranium diffusion in the uranium sublattice is relatively low (+1.8 eV) compared to the energy required to form a Schottky defect (+4.3 eV). This feature supports the conclusions of Matsui and Matzke,[9] who associate from experimental considerations the values of 2.4 and 3.7 eV for migration and formation energy, respectively. From this paper, this repartition of about 1/3 is compatible with results obtained on refractory metals. For these two sets of values, the sum of the formation and migration energies is about +6.1 eV in agreement with the value measured by Matzke *et al.*[5] in the case of a pure single crystal of UC. Slightly higher values (+6.8 eV) were also measured by Matthews[10] and Sarian and Dalton.[46]

(b) A second possible diffusion path for uranium atoms is based on a mechanism involving uranium diffusion through interstitial sites.[8] For this mechanism, uranium vacancies must be associated with uranium interstitials in uranium Frenkel pairs to respect stoichiometry. However, the formation energy of the uranium Frenkel pair is too high (+7.6 eV) and this interstitial mechanism cannot constitute a plausible alternative to the diffusion of uranium atoms in the cell.

(c) The diffusion of uranium atoms through the carbon sublattice as mentioned by Catlow[8] should be favored by the significant concentration of carbon vacancies in the lattice. Chartier and Van Brutzel[14] tested Catlow's assumptions using molecular dynamics and found that the largest part of the activation energy is due to the migration energy, i.e., +6.6 eV, against +0.75 eV for the formation energy. The high migration energy when an atom moves onto an adjacent vacant carbon site is related to the formation of a vacancy on the uranium sublattice. A schematic energy curve corresponding to this diffusion path is shown in Fig. 6. In order to compare with Chartier's results, we computed energies associated with intermediate positions labeled "states 1" and "states 2" and corresponding to a composition-conserving clustering defect coupling the dimer C_2, uranium in an antisite, and a uranium vacancy defect. The energy of this cluster was calculated by summing the energies of the isolated defects composing it. We find that the energy of states 1 is 6.0 eV higher than the energy of the initial state. The saddle points between the different states have not been determined accurately but as schematized in Fig. 6, we estimate that they are relatively low compared to energies of states 1 and 2. In a first approximation, the estimated energy for this diffusion path should be greater than 6.9 eV when the initial state energy (+0.9 eV) associated with the formation of the "$C_2 + \square^C$" defect is included in the balance. A good accordance with Chartier's results (+7.35 eV) can be noted.

(d) This last mechanism supposes that atoms jump from uranium sites toward vacant sites on the carbon sublattice. This one does not take into account the amount of uranium

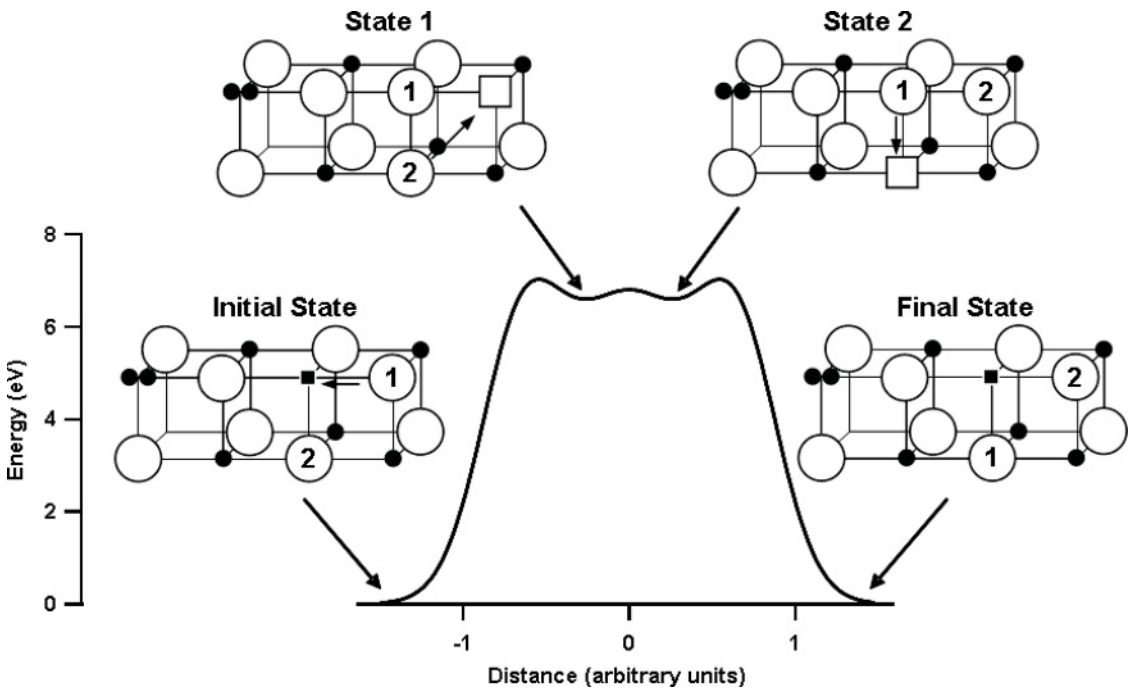

FIG. 6. Energy path for uranium diffusion through carbon sublattice and structure of initial state, intermediate transition states, and final state.

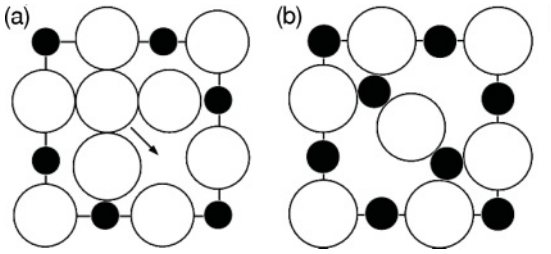

FIG. 7. Uranium diffusion path according to the two mechanisms proposed here. (a) Diffusion through carbon sublattice. (b) Saddle position of uranium atom along the diffusion path inside the uranium sublattice.

atoms that could be naturally present in antisites on the carbon sublattice under the effect of thermal disorder. Also, in such a situation, it is not necessary to take into account the energy for creating uranium vacancies. However, to keep constant composition in the crystal, we should include two dimers C_2 (3.0 eV are needed). This complex defect corresponds to the triple defect described in Sec IV. Such a defect allows the saving of +0.4 eV compared to the energy required to form a Schottky defect, the main contributor of uranium vacancy defects in the cell. Here, diffusion occurs via carbon vacancies for which the concentration is controlled by the thermally activated defect $C_2 + \square^C$. The activation energy calculated for this mechanism is nevertheless slightly higher than for the process based on a uranium vacancy (+6.6 against 6.1 eV) due to a migration energy higher (+2.7 eV; see Table VI) than that required for the diffusion of uranium via the uranium sublattice (+1.8 eV).

Our findings show that diffusion of uranium can be relatively complex (Fig. 7). The likely mechanism for uranium diffusion occurs through uranium sublattice vacancies. Reasonably, we cannot exclude the fact that diffusion can occur through carbon vacancies but at stoichiometry, this mechanism requires that a certain quantity of uranium in antisites is formed in triple defects with C_2 dimers. We show in the following that this mechanism is most favorable in the understoichiometric regime because antisite defects coupled with carbon vacancies are used to accommodate the understoichiometry and are, therefore, preexisting in the cell.

2. *Off-stoichiometric compositions*

Unlike the stoichiometric composition for which only thermal defects are present, the alloys with off-stoichiometric compositions may have constitutional defects that can participate in and influence the migration of atoms.

a. Understoichiometry. We have seen in the previous section that the dominant defects for understoichiometric composition are constituted by carbon vacancies in association with uranium in antisites. We can estimate that in this case, the uranium in antisites should diffuse preferentially through the carbon sublattice, especially if the uranium atom in the antisite is coupled with one carbon vacancy in an adjacent position. The migration energy associated with this mechanism is calculated as +2.7 eV. We can conclude that uranium migration is governed by carbon sublattice diffusion due to the large concentration of uranium antisite defects in the lattice and the low migration energy needed for uranium to move to an adjacent carbon vacancy. The calculated value for this mechanism (+2.7 eV) is very close to that measured by Lindner*et al.*[13] for understoichiometric composition (+3 eV). Other authors like Hirsch and Scherff[12] nevertheless measure higher activation energies for uranium diffusion in the understoichiometric domain of the UC phase diagram. This divergence might be explained by the fact that the diffusion process can also occur via Schottky defects produced as the temperature increases.

By the molecular dynamics method, Chartier[14] calculated the activation energy for uranium diffusion in the understoichiometric regime by assuming on the model of the scheme presented in the Fig. 6 that the uranium atom diffuses toward carbon vacancies (in Chartier's scenario, uranium antisites are not identified as constitutional defects). The uranium vacancy created after the uranium jump to an adjacent carbon vacancy contributes in large part to the high activation energy of this model. This value is treated with caution because of the experimental value reported by Catlow[8] from Matthews's work[10] but wrongly, because understoichiometry is not treated by this author. In contrast, Matzke[1] shows from reviewing work based on a series of experimental studies that activation energy for the understoichiometric regime is much lower than that reported by Catlow, which supports the existence of constitutional uranium antisite defects.

b. Overstoichiometry. For overstoichiometric compositions, the C_2 dimer is predicted to be the most favorable defect. In contrast to the understoichiometric regime, this dominant defect should not participate in uranium diffusion; at most it can constitute a barrier to the migration. As for the stoichiometric composition, we can estimate that uranium diffusion occurs through the uranium vacancies, thermally formed with the Schottky defects. The activation energy should have the same value as that calculated for the stoichiometric composition and is estimated to 6.1 eV. Nevertheless, experimental works show that the activation energy for the uranium atom increases linearly in the overstoichiometric region up to a step value for a C:U ratio of 1.07,[1,47] for which the activation energy is +7.6 eV. Such a behavior can be related to the increase of C_2 dimers in the crystal which has the effect of increasing mechanical stress inside the lattice. We estimate that the migration energy should be affected by the excess of dimers even if uranium atoms do not diffuse via the carbon sublattice.

VI. CONCLUSION

A theoretical study of the migration of uranium and carbon atoms in UC using the DFT-GGA framework has been proposed. Despite the inherent difficulties related to the DFT formalism in treating the case of 5*f* electrons of uranium, our calculations of the activation energies of diffusion processes for the different regimes of composition agree very well with experimental data.

In the first step, our calculations of single-defect formation energies provide important results. Compared to a previous study,[25] we show the important role of the uranium antisite defect in the understoichiometric regime. In the overstoichiometric regime, C_2 dimers are the most stable defects. The participation of C_2 dimers as composition-conserving defects

when combined with carbon vacancies is considered as the dominant source of thermal defects. The analysis of defect energies leads to definition of the preponderant population of defects for each regime of composition, which is fundamental in the understanding of migration mechanisms in $UC_{1\pm x}$. Such calculations have been performed within a formalism taking into account the composition variation induced by defects in the cell.

In the second step, the calculated formation energies of single and complex defects as well as migration energies calculated by the NEB method allow us to propose preferential paths for diffusion of atoms that can be summarized as follows.

For carbon atoms:

(a) At stoichiometric composition, the diffusion of carbon operates both through the carbon vacancies of thermal defects formed with C_2 dimers and by an interstitial path from the doubly occupied octahedral sites toward singly occupied carbon sites ($E_a = 2.5$–2.9 eV).

(b) For understoichiometric compositions, the carbon diffuses preferentially from the carbon vacancies of the complex defects formed with uranium in antisites ($E_a = 2$ eV).

(c) For overstoichiometric compositions, the dominant defects are C_2 dimers; the diffusion occurs through an interstitial mechanism from dimer sites by a mechanism similar to those occurring at the stoichiometric composition ($E_a = 1.6$ eV).

For uranium atoms:

(a) At stoichiometry, uranium atoms diffuse preferentially via the uranium vacancies generated by the Schottky defects ($E_a = 6.1$ eV) even though a mechanism through the carbon sublattice cannot be excluded because of the low energy required to place uranium on a carbon site (antisite).

(b) In the understoichiometric region, uranium atoms placed in antisites to accommodate the stoichiometric deviation diffuse on the carbon sublattice with an energy lower by half (2.7 eV) than for stoichiometric and overstoichiometric compositions.

(c) For overstoichiometry the diffusion is ensured by Schottky defects as for the stoichiometric case.

Note that these results constitute a preliminary study before addressing the issue of the incorporation and migration of fission products that will be done in the continuation of this work. Let us also emphasize that molecular dynamics simulations should be undertaken on the basis of this work to study the specific behavior of fission cascades or gas resolution in UC irradiated materials as was previously done for uranium dioxide.[48,49]

*roland.ducher@irsn.fr

[1] Hj. Matzke, J. Less-Common Met. **121**, 537 (1986).
[2] M. S. Veshchunov, J. Nucl. Mater. **277**, 67 (2000).
[3] M. S. Veshchunov, R. Dubourg, V. V. Ozrin, V. E. Shestak, and V. I. Tarasov, J. Nucl. Mater. **362**, 327 (2007).
[4] M. S. Veshchunov and V. E. Shestak, J. Nucl. Mater. **384**, 12 (2009).
[5] Hj. Matzke, J. L. Routbort, and H. A. Tasman, J. Appl. Phys. **45**, 5187 (1974).
[6] S. Sarian, J. Nucl. Mater. **49**, 291 (1973).
[7] Y. Makino, P. Son, M. Miyake, and T. Sano, J. Nucl. Mater. **49**, 225 (1973).
[8] C. R. A. Catlow, J. Nucl. Mater. **60**, 151 (1976).
[9] H. Matsui and Hj. Matzke, J. Nucl. Mater. **89**, 41 (1980).
[10] J. R. Matthews, UKAEA Report No. AERE-M2643, 1974 (unpublished).
[11] W. Schule and P. Spindler, J. Nucl. Mater. **32**, 20 (1969).
[12] H. J. Hirsch and H. L. Scherff, J. Nucl. Mater. **45**, 123 (1972).
[13] R. Lindner, G. Riemer, and H. L. Scherff, J. Nucl. Mater. **23**, 222 (1967).
[14] A. Chartier and L. Van Brutzel, Nucl. Instrum. Methods Phys. Res., Sect. B **255**, 146 (2007).
[15] T. Petit, C. Lemaignan, F. Jollet, B. Bigot, and A. Pasturel, Philos. Mag. B **77**, 779 (1998).
[16] J. P. Crocombette, F. Jollet, L. Thien Nga, and T. Petit, Phys. Rev. B **64**, 104107 (2001).
[17] J. P. Crocombette, J. Nucl. Mater. **305**, 29 (2002).
[18] M. Freyss, T. Petit, and J. P. Crocombette, J. Nucl. Mater. **347**, 44 (2005).
[19] F. Gupta, G. Brillant, and A. Pasturel, Philos. Mag. **87**, 2561 (2007).
[20] H. Y. Geng, Y. Chen, Y. Kaneta, M. Iwasawa, T. Ohnuma, and M. Kinoshita, Phys. Rev. B **77**, 104120 (2008).
[21] G. Brillant and A. Pasturel, Phys. Rev. B **77**, 184110 (2008).
[22] F. Gupta, A. Pasturel, and G. Brillant, J. Nucl. Mater. **385**, 368 (2009).
[23] L. Petit, A. Svane, Z. Szotek, W. M. Temmerman, and G. M. Stocks, Phys. Rev. B **80**, 045124 (2009).
[24] H. Shi, P. Zhang, S. S. Li, B. Sun, and B. Wang, Phys. Lett. A **373**, 3577 (2009).
[25] M. Freyss, Phys. Rev. B **81**, 014101 (2010).
[26] J. Trygg, J. M. Wills, M. S. S. Brooks, B. Johansson, and O. Eriksson, Phys. Rev. B **52**, 2496 (1995).
[27] T. Ejima, K. Murata, S. Suzuki, T. Takahashi, S. Sato, T. Kasuya, Y. Onuki, H. Yamagami, A. Hasegawa, and T. Ishii, Physica B **186-188**, 77 (1993).
[28] M. S. Veshchunov, V. V. Ozrin, V. E. Shestak, V. I. Tarasov, R. Dubourg, and G. Nicaise, Nucl. Eng. Des. **236**, 179 (2006).
[29] G. Kresse and D. Joubert, Phys. Rev. B **59**, 1758 (1999).
[30] G. Kresse and J. Furthmuller, Comput. Mater. Sci. **6**, 15 (1996).
[31] Y. Wang and J. P. Perdew, Phys. Rev. B **44**, 13298 (1991).
[32] L. Brewer, Lawrence Berkeley Laboratory Report No. LBL-3720, 1977 (unpublished).
[33] G. Henkelman, A. Arnaldsson, and H. Jonsson, Comput. Mater. Sci. **36**, 254 (2006).
[34] J. S. Olsen, L. Gerward, U. Benedict, J. P. Itié, and K. Richter, J. Less-Common Met. **121**, 445 (1986).
[35] P. Y. Chevalier and E. Fischer, J. Nucl. Mater. **288**, 100 (2001).
[36] S. L. Dudarev, D. Nguyen Manh, and A. P. Sutton, Philos. Mag. B **75**, 613 (1997).
[37] A. L. Bowman, G. P. Arnold, W. G. Witteman, T. C. Wallace, and N. G. Nereson, Acta Crystallogr. **21**, 670 (1966).
[38] P. A. Korzhavyi, A. V. Ruban, A. Y. Lozovoi, Yu. Kh. Vekilov, I. A. Abrikosov, and B. Johansson, Phys. Rev. B **61**, 6003 (2000).
[39] Y. Mishin and D. Farkas, Philos. Mag. A **75**, 169 (1997).

[40]F. Jeanne, Thesis, Université Scientifique et Médicale de Grenoble, 1972.
[41]T. C. Wallace, W. G. Witterman, C. L. Radesevich, and M. G. Bowman, Los Alamos Scientific Laboratory Report No. LA-DC 8840, 1968 (unpublished).
[42]R. A. Krakowski, J. Nucl. Mater. **32**, 120 (1969).
[43]Y. Bertaud, Commissariat à l'énergie atomique Report No. CEA-R-4227, 1971 (unpublished).
[44]G. G. Bentle and G. Ervin Jr., USAEC Report No. AI-12726, Atomics International, 1968 (unpublished).
[45]H. M. Lee and L. R. Barret, J. Nucl. Mater. **27**, 275 (1968).
[46]S. Sarian and J. T. Dalton, J. Nucl. Mater. **48**, 351 (1973).
[47]J. L. Routbort and R. N. Singh, J. Nucl. Mater. **58**, 78 (1975).
[48]D. C. Parfitt and R. W. Grimes, J. Nucl. Mater. **381**, 216 (2008).
[49]D. C. Parfitt and R. W. Grimes, J. Nucl. Mater. **392**, 28 (2009).